Electronic Supplementary Material (ESI) for Dalton Transactions.

Probing Ferroic Transitions in a Multiferroic Framework Family: A Neutron Diffraction Study of the Ammonium Transition Metal Formates

James M. M. Lawler,[a] Pascal Manuel,[b] Amber L. Thompson[a] and Paul J. Saines[a]

[a] Department of Chemistry, University of Oxford, Inorganic Chemistry Laboratory, South Parks Road, Oxford, OX1 3QR, United Kingdom

b ISIS Facility, Rutherford Appleton Laboratory, Harwell, Didcot OX11 0QX, United Kingdom

Experimental

Synthesis

All reagents were available commercially and used without further purification. In a typical reaction 10 mL of 0.4 M $MCl_2 \cdot xH_2O$ (x = 4, 4, 0 and 6 for Mn2+, Fe^{2+}, Co^{2+} and Ni^{2+}, respectively) in methanol solution was layered on top of 10 mL of 1.6 M $(NH_4)(HCO_2)$ (99.995 %), and 0.8 M H_2CO_2 (95 %) in methanol solution. Additionally, in the synthesis of the Fe^{2+} framework, 100 mg of ascorbic acid was added to the top layer to reduce the oxidation of Fe^{2+} to Fe^{3+}. Samples were harvested by filtration from the reactions within a week in the form of single crystals, or in the case of $NH_4Ni(HCO_2)_3$, microcrystallites. Yields of over 80 %, as a percentage of the metal used, were obtained for the Mn^{2+}, Co^{2+} and Ni^{2+} phases while the maximum obtained for the Fe^{2+} phase was 55 %. Crystal, suitable for single crystal diffraction, of a new polymorph of the $NH_4Mn(HCO_2)_3$ phase were obtained from a layered reaction using 0.2 M $MnCl_2 \cdot 4H_2O$ methanol solution layered on a methanol solution of 0.8 M $(NH_4)(HCO_2)$ and 0.3 M H_2CO_2.

Rietveld Refinement Restraints and Constraints

Refinements were carried out with a time-of-flight peak profile function featuring a convolution of back-to-back exponentials with a pseudo-Voigt function (GSAS profile 3) with backgrounds modeled using shifted Chebyschev polynomials. In fits of the $P6_322$ high temperature phase to the neutron diffraction data soft restraints were applied to hold the N-D bond distances near to 1.0 Å. Additional restraints were also applied when refining the lower symmetry $P6_3$ phase to ensure the formate anion also retained reasonable geometry with C-D and C-O soft bond distance restraints of 1.0 and 1.2 Å. Displacement parameters of all atoms were all refined isotropically with atoms of the same type constrained to be equal across all phases in a refinement, except the thermal parameters of the D which were split into two groups depending on whether they were part of the ligand or in the channels of the structures. Additionally, due to the very weak Co^{2+} neutron scattering length, the displacement parameter of the Co^{2+} sites in $(ND_4)Co(DCO_2)_3$ were constrained to be equal to the O atoms to which they are bonded. The occupancies of the D sites were refined against the highest temperature patterns collected of each compound to determine the extent of deuteration with occupancies constrained into two groups depending on whether they are part of formate ligands or more labile groups such as ammonia. These refined values were then kept fixed in all other refinements for each compound as it was considered unlikely chemically that they would change, indeed attempts to refine these values against low temperature datasets did not indicate any significant changes with temperature. The atomic parameters of impurity phases were refined at high temperature to ensure their deuterium positions were determined accurately and then fixed in lower temperature refinements due to the small amount of these present leading to lower precision refinements.

Results

New Polymorph Description

The new $NH_4B(HCO_2)_3$ polymorph adopts a polar $Pna2_1$ orthorhombic structure at 150 K (see compound 1 in Table S1 for crystallographic parameters). The asymmetric unit features one Mn^{2+} cation, one NH_4^+ molecule and three formate ligands. All formate ligands, which have typical geometry, bond to one Mn^{2+} cation through each oxygen atom in a *syn-anti* mode. The

Mn^{2+} cations have a bond valence of 2.05 in a slightly distorted octahedral geometry.[1] Overall the framework structure is isostructural with $NH_4Cd(HCO_2)_3$ and appears to be close to a heavily distorted ReO_3 structure.[2] The MnO_6 octahedra in adjacent layers along the *b* and *c*-axis are, however, offset by half a unit cell along *a* (see Fig. 1a). Additionally there appear to be two types of channels in the structure when viewed down the *a*-axis, the larger of which is doubly occupied by ammonium molecules to maintain ABX_3 stoichiometry. The hydrogen atoms from the formate molecules protrude into the smaller channel rendering it far too small to contain any guest molecules. The polar nature of the structure appears to primarily originate from the alignment of the ammonia molecules along the *c*-axis. As for many other $AB(HCO_2)_3$ frameworks it is possible the structure undergoes a order-disorder transition at higher temperatures but this has not been investigated further.[3]

Table S1 Crystallographic Data for structures **1-3** determined by single crystal X-ray diffraction.

Compound	**1**	**2**	**3**
Formula	$\mathrm{Mn_1C_3H_7N_1O_6}$	$\mathrm{Mn_1C_3H_7N_1O_6}$	$\mathrm{Co_1C_3H_7N_1O_6}$
Formula Weight	208.02	208.02	212.02
T (K)	150(2)	30(2)	30(2)
Crystal System	Orthorhombic	Hexagonal	Hexagonal
Space Group	$Pna2_1$ (33)	$P6_3$	$P6_3$
a (Å)	6.8568(2)	12.65088(13)	12.5965(2)
b (Å)	9.3906(2)	12.65088(13)	12.5965(2)
c (Å)	10.7307(3)	8.54951(9)	8.2395(1)
α (°)	90	90	90
β (°)	90	90	90
γ (°)	90	120	120
V (Å^3)	690.94(3)	1184.987(12)	1132.221(14)
Z	4	6	6
ρ_{calc} (g cm^{-3})	2.000	1.749	1.866
μ (cm^{-1})	1.895	1.657	2.259
Refl. Meas./Unique	9149/1481 [R_{int} = 0.045]	26983/2878 [R_{int} = 0.044]	25583/2729 [R_{int} = 0.058]
Parameters Refined	101	131	131
$R1$, $wR2^{\mathrm{a}}$ (all)	0.0327, 0.0641	0.0388, 0.0744	0.0432, 0.0737
$R1$, $wR2^{\mathrm{a}}$ (obs)	0.0275, 0.0617	0.0351, 0.0702	0.0317, 0.0594
χ^2	0.9596	0.9457	0.9563

[a] $w = 1/[\sigma^2(F_o^2) + (aP)^2 + bP]$ and $P = \left(\max(F_o^2, 0) + 2F_c^2\right)/3$; $R1 = \sum||F_o| - |F_c||/\sum|F_o|$ and

$$wR2 = \sqrt{\left\{\sum\left[w\left(F_o^2 - F_c^2\right)^2\right]/\sum w\left(F_o^2\right)^2\right\}}$$

Table S2 Crystallographic details of $ND_4Mn(DCO_2)_3$ determined from neutron diffraction data collected at 300 K. Final total refinement statistics R_p and R_{wp} were 2.78 % and 3.93 %.

Space Group	*a* (Å)	*b* (Å)	*c* (Å)	Volume (Å^3)	
$P6_322$	7.36189(14)	7.36189(14)	8.50283(20)	399.091(14)	
Site	x	y	z	U$_{iso}$ (Å^2)	Fractional Occupancy
Mn1	1/3	2/3	1/4	0.018(3)	1
N1	0	0	0.2257(13)	0.0237(18)	0.5
O1	0.0998(3)	0.7023(3)	0.1055(2)	0.0190(6)	1
C1	0	0.5651(6)	0	0.0623(16)	1
D1	0	0.4422(6)	0	0.125(3)	1
D2	0.0228(11)	0.8904(9)	0.1814(5)	0.0197(2)	0.344(2)
D3	0	0	0.1605(13)	0.0197(2)	0.344(2)

Table S3 Crystallographic details of $ND_4Mn(DCO_2)_3$ determined from neutron diffraction data collected at 30 K. Final total refinement statistics R_p and R_{wp} were 3.55% and 4.32 %.

Space Group	*a* (Å)	*b* (Å)	*c* (Å)	Volume (Å^3)	
$P6_3$	12.6667(2)	12.6667(2)	8.56535(19)	1190.16(4)	
Site	x	y	z	U$_{iso}$ (Å^2)	Fractional Occupancy
Mn1	0.335(3)	0.334(3)	0.613(3)	-0.005(3)	1
C1	0.3771(14)	0.1884(13)	0.337(3)	0.0127(5)	1
C2	0.4622(11)	0.5188(12)	0.324(3)	0.0127(5)	1
C3	0.1394(16)	0.2931(15)	0.362(3)	0.0127(5)	1
N1	2/3	1/3	0.54944	0.0009(12)	1
N2	1/3	2/3	0.543(4)	0.0009(12)	1
N3	0	0	0.151(2)	0.0009(12)	1
O1	0.4294(14)	0.2567(14)	0.458(3)	0.0004(6)	1
O2	0.4429(15)	0.1634(18)	0.249(3)	0.0004(6)	1
O3	0.3984(14)	0.4927(16)	0.453(3)	0.0004(6)	1
O4	0.4882(15)	0.6084(13)	0.234(3)	0.0004(6)	1
O5	0.1737(15)	0.2384(13)	0.454(3)	0.0004(6)	1
O6	0.0651(13)	0.2404(16)	0.251(3)	0.0004(6)	1
D1	0.2839(15)	0.1570(13)	0.314(3)	0.0254(11)	1
D2	0.4898(12)	0.4555(12)	0.300(3)	0.0254(11)	1
D3	0.1676(17)	0.3826(16)	0.397(4)	0.0254(11)	1
D11	0.5858(11)	0.3142(17)	0.504(3)	0.0036(14)	0.687
D12	2/3	1/3	0.6657(6)	0.0036(14)	0.687
D21	0.3612(20)	0.6087(16)	0.511(3)	0.0036(14)	0.687
D22	1/3	2/3	0.659(4)	0.0036(14)	0.687
D31	0.0329(20)	0.0869(10)	0.188(4)	0.0036(14)	0.687
D32	0	0	0.035(2)	0.0036(14)	0.687

Table S4 Crystallographic details of $ND_4Co(DCO_2)_3$ determined from neutron diffraction data collected at 250 K. Final total refinement statistics R_p and R_{wp} were 2.57 % and 3.47 %.

Space Group	*a* (Å)	*b* (Å)	*c* (Å)	Volume (Å^3)	
$P6_322$	7.29959(12)	7.29959(12)	8.20227(15)	378.497(11)	
Site	x	y	z	U$_{iso}$ (Å^2)	Fractional Occupancy
Co1	1/3	2/3	1/4	0.0074(5)	1
N1	0	0	0.2209(10)	0.0351(13)	0.5
O1	0.10381(21)	0.69317(18)	0.10434(15)	0.0074(4)	1
C1	0	0.5588(3)	0	0.0363(5)	1
D1	0	0.4214(3)	0	0.0726(11)	1
D2	0.0343(7)	0.8908(6)	0.1848(4)	0.0233(15)	0.376(1)
D3	0	0	0.1625(10)	0.0233(15)	0.376(1)

Table S5 Crystallographic details of $ND_4Co(DCO_2)_3$ determined from neutron diffraction data collected at 20 K. Final total refinement statistics R_p and R_{wp} were 2.63% and 3.29 %.

Space Group	*a* (Å)	*b* (Å)	*c* (Å)	Volume (Å^3)	
$P6_3$	12.59646(17)	12.59646(17)	8.23953(13)	1132.22(3)	
Site	x	y	z	U$_{iso}$ (Å^2)	Fractional Occupancy
Co1	0.3407(12)	0.3318(13)	0.59072	0.0004(4)	1
C1	0.3703(9)	0.1842(10)	0.3246(17)	0.00901(34)	1
C2	0.4727(9)	0.5177(10)	0.3274(16)	0.00901(34)	1
C3	0.1444(9)	0.2936(10)	0.3543(16)	0.00901(34)	1
N1	2/3	1/3	0.532(3)	0.0210(10)	1
N2	1/3	2/3	0.546(2)	0.0210(10)	1
N3	0	0	0.128(2)	0.0210(10)	1
O1	0.4299(11)	0.2697(9)	0.4371(18)	0.0008(4)	1
O2	0.4331(10)	0.1595(10)	0.2329(19)	0.0008(4)	1
O3	0.3905(10)	0.4912(8)	0.4427(19)	0.0008(4)	1
O4	0.4971(11)	0.5914(9)	0.2220(18)	0.0008(4)	1
O5	0.1770(10)	0.2408(9)	0.4470(18)	0.0008(4)	1
O6	0.0806(8)	0.2520(9)	0.2399(18)	0.0008(4)	1
D1	0.2704(9)	0.1533(8)	0.3024(17)	0.0180(7)	0.7520
D2	0.5061(9)	0.4571(9)	0.2921(18)	0.0180(7)	0.7520
D3	0.1960(11)	0.3931(10)	0.3435(18)	0.0180(7)	0.7520
D11	0.5783(8)	0.3087(12)	0.4955(18)	0.0080(9)	0.7520
D12	2/3	1/3	0.655(3)	0.0080(9)	0.7520
D21	0.3584(13)	0.6112(12)	0.4877(19)	0.0080(9)	0.7520
D22	1/3	2/3	0.667(3)	0.0080(9)	0.7520
D31	0.0331(12)	0.0960(10)	0.1525(18)	0.0080(9)	0.7520
D32	0	0	0.002(3)	0.0080(9)	0.7520

Table S6 Crystallographic details of $ND_4Ni(DCO_2)_3$ determined from neutron diffraction data collected at 250 K. Final total refinement statistics R_p and R_{wp} were 2.58% and 3.71 %.

Space Group	*a* (Å)	*b* (Å)	*c* (Å)	Volume (Å^3)	
$P6_322$	7.2827(2)	7.2827(2)	8.0532(3)	369.89(2)	
Site	x	y	z	U_{iso} (Å^2)	Fractional Occupancy
Ni1	1/3	2/3	1/4	0.0144(7)	1
N1	0	0	0.2262(11)	0.0438(12)	0.5
O1	0.10905(20)	0.69113(19)	0.10519(18)	0.0038(4)	1
C1	0	0.5585(4)	0	0.0316(5)	1
D1	0	0.4184(4)	0	0.0632(11)	0.990(7)
D2	0.0397(10)	0.8974(9)	0.1764(5)	0.044(3)	0.299(3)
D3	0	0	0.1525(11)	0.044(3)	0.299(3)

Table S7 Crystallographic details of $ND_4Ni(DCO_2)_3$ determined from neutron diffraction data collected at 40 K. Final total refinement statistics R_p and R_{wp} were 2.92% and 3.45 %.

Space Group	*a* (Å)	*b* (Å)	*c* (Å)	Volume (Å^3)	
$P6_322$	7.26363(19)	7.26363(19)	8.0693(2)	368.702(17)	
Site	x	y	z	U_{iso} (Å^2)	Fractional Occupancy
Ni1	1/3	2/3	1/4	0.0027(5)	1
N1	0	0	0.2154(6)	0.0285(9)	0.5
O1	0.11017(14)	0.69130(14)	0.10547(11)	0.0014(3)	1
C1	0	0.55840(18)	0	0.0156(2)	1
D1	0	0.41314(17)	0	0.0312(5)	0.990
D2	0.0390(6)	0.8889(6)	0.1656(3)	0.0189(12)	0.299
D3	0	0	0.1600(8)	0.0189(12)	0.299

Supplementary Figures

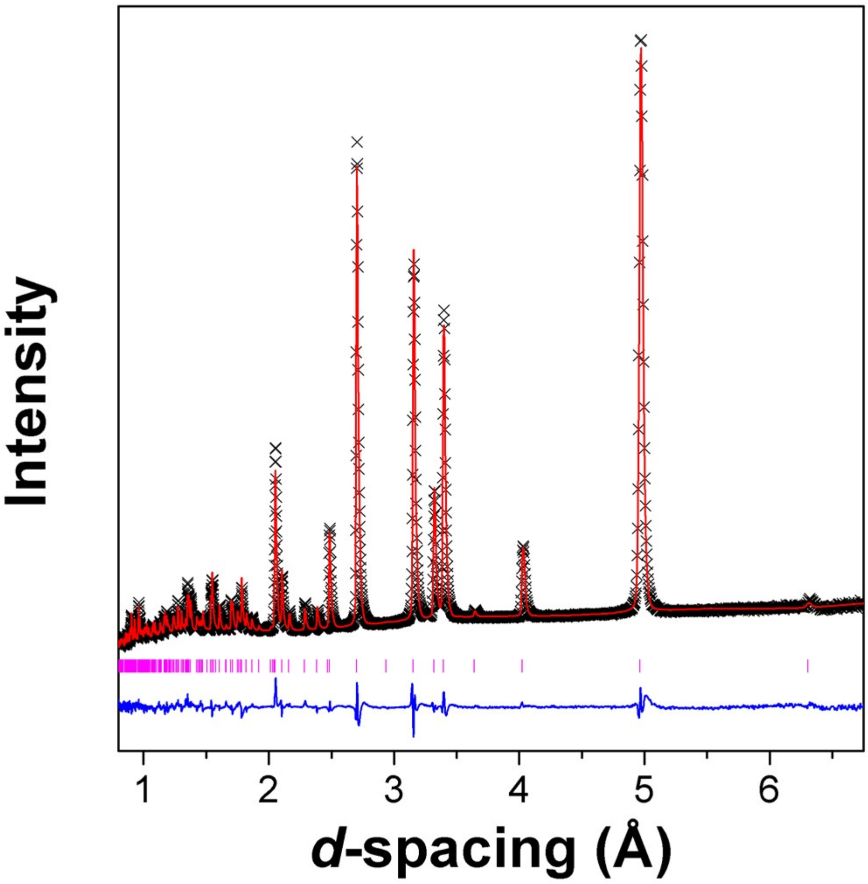

Fig. S1 Powder neutron diffraction patterns of $ND_4Ni(DCO_2)_3$ collected at 250 K using banks 3 and 7 of the high resolution WISH diffractometer. The observed data are represented by black crosses and the upper red and lower blue lines are the calculated and difference plots respectively. The magenta vertical reflection markers are the expected Bragg reflections from the $P6_322$ phase.

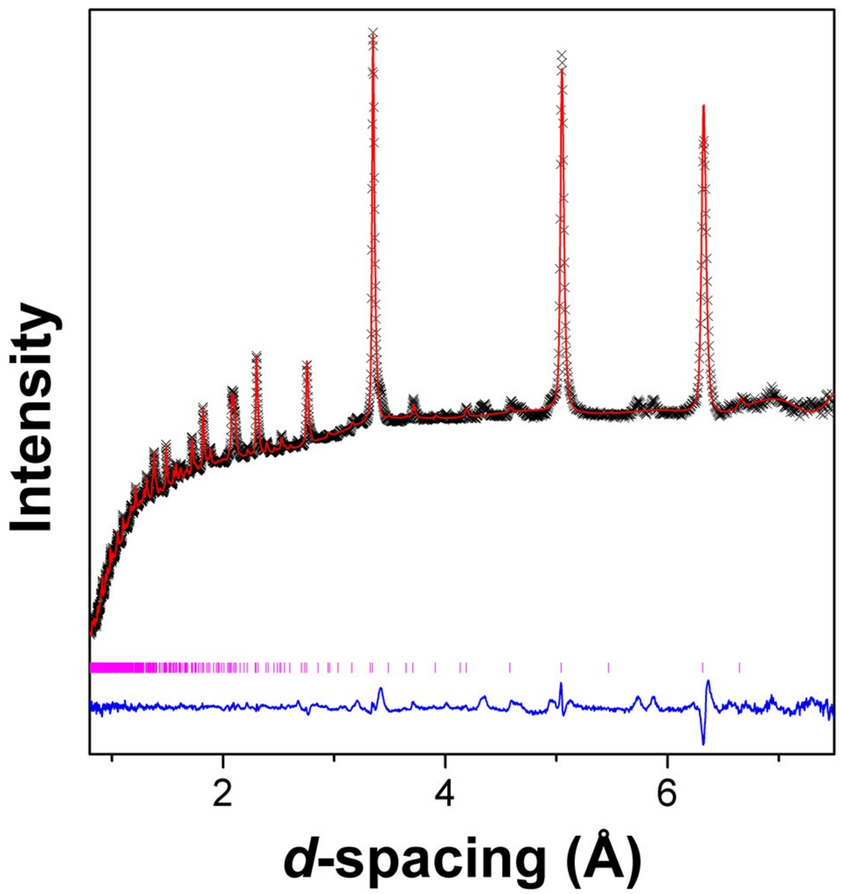

Fig. S2 Powder neutron diffraction patterns of $NH_4Fe(HCO_2)_3$ collected at 20 K using banks 3 and 7 of the high resolution WISH diffractometer. The format is the same as for Fig. S1. The Bragg reflection markers are those from the *P*6_3 phase.

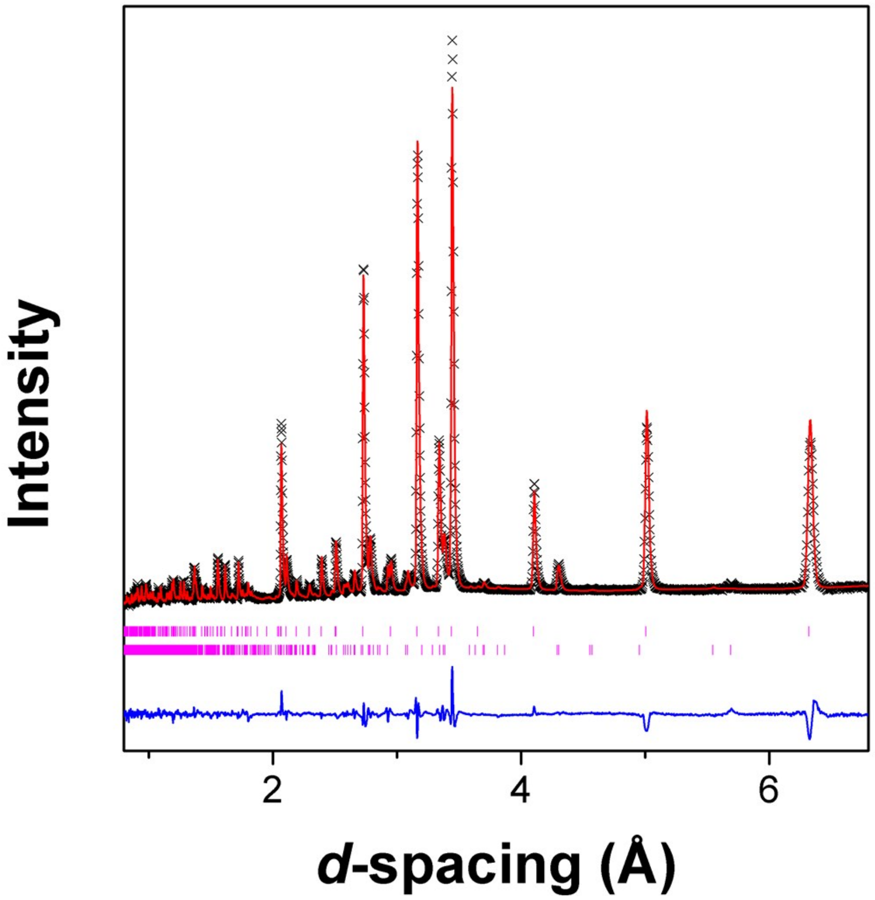

Fig. S3 Powder neutron diffraction patterns of $ND_4Co(DCO_2)_3$ collected at 250 K using banks 3 and 7 of the high resolution WISH diffractometer. The format is the same as Fig. S1. The upper and lower markers Bragg reflections markers are those of the $P6_3$ phase and $Co(DCO_2)_2{\cdot}2(D_2O)$ impurity.[5]

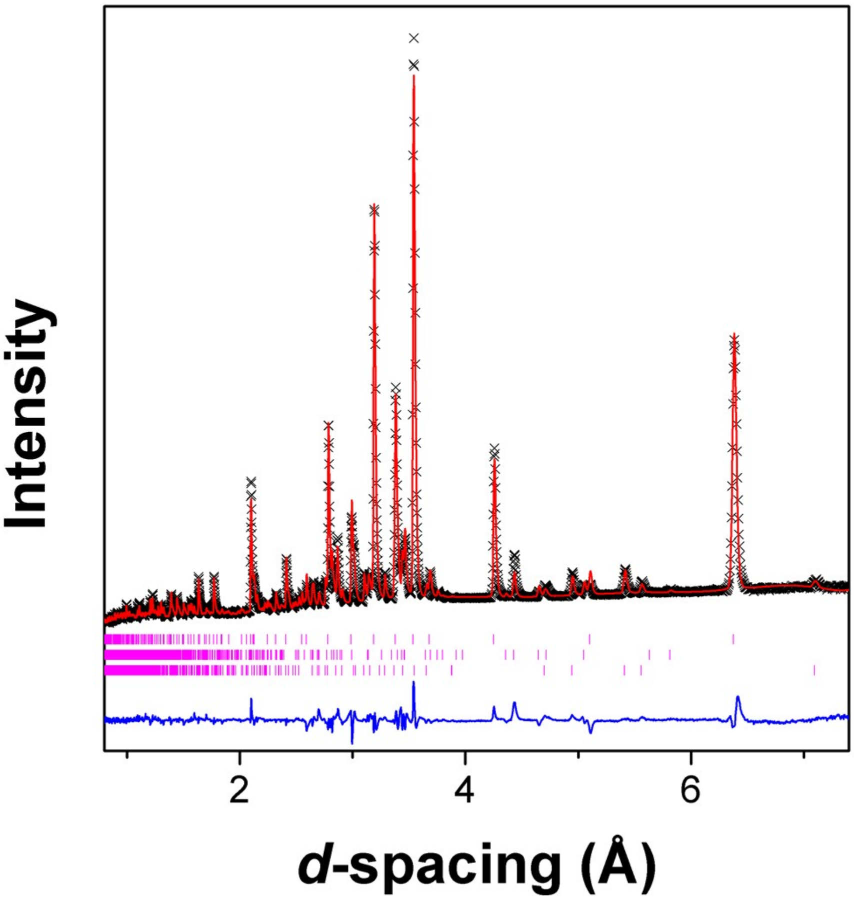

Fig. S4 Powder neutron diffraction patterns of $ND_4Mn(DCO_2)_3$ collected at 300 K using banks 3 and 7 of the high resolution WISH diffractometer. The format is the same as Fig. S1. The upper, middle and lower markers Bragg reflections markers are those of the *P*6_3 phase and the $Mn(DCO_2)_2 \cdot 2(D_2O)$[5] and new $ND_4Mn(DCO_2)_3$ impurities.

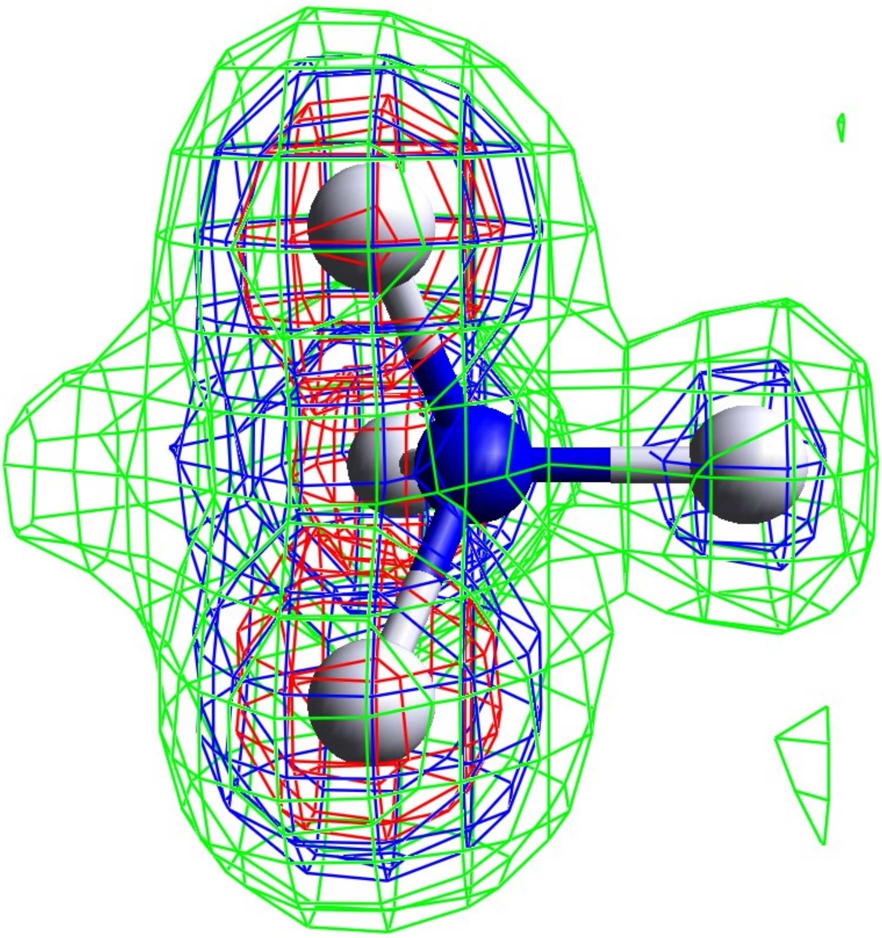

Fig. S5 Fourier electron density difference map in the region surrounding the N(3)H_4 cations in the low temperature $NH_4Co(HCO_2)_3$ phase. This was obtained from fits to synchrotron X-ray diffraction data at 30 K.

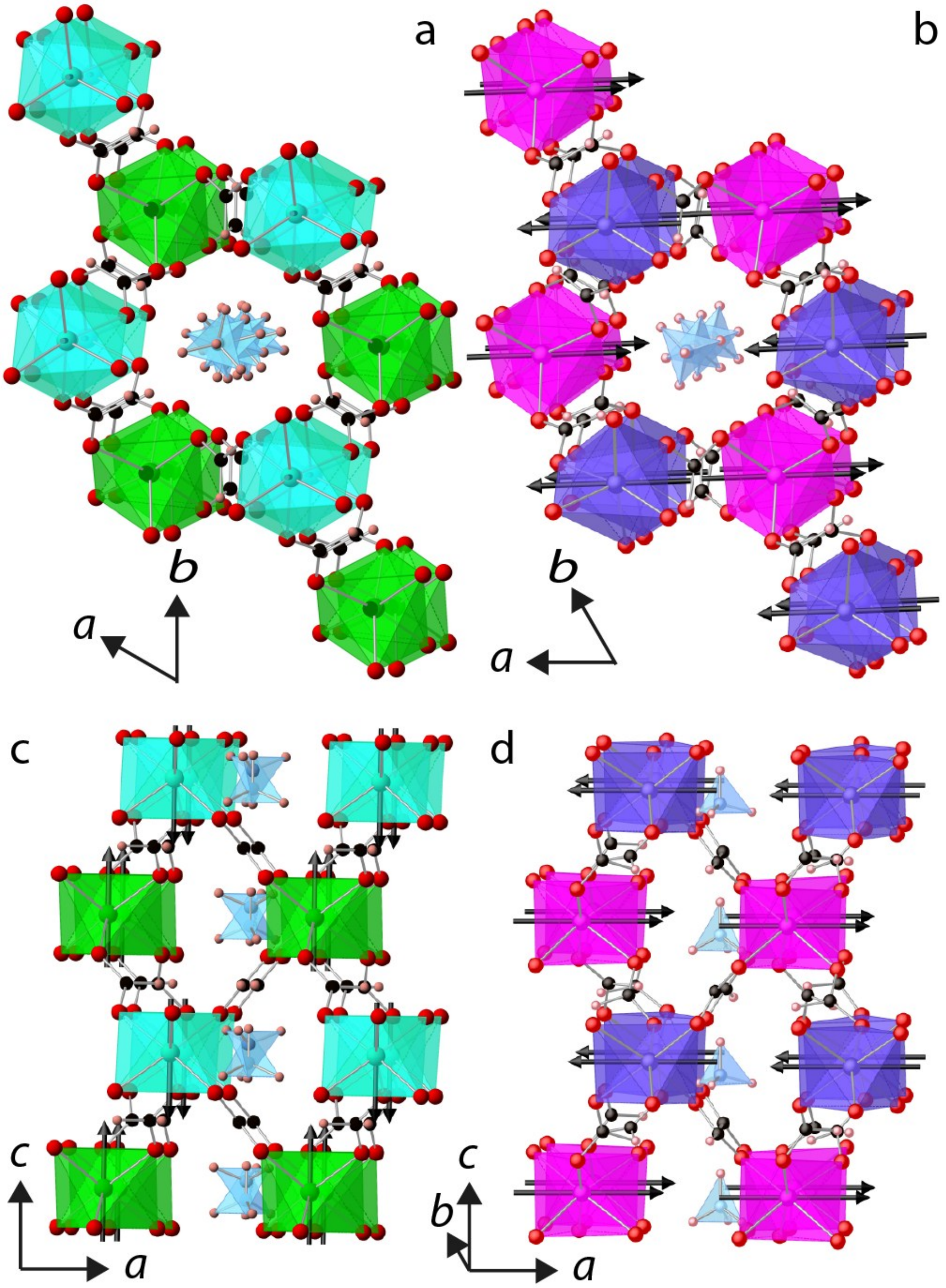

Fig. 6 Magnetic structures of $ND_4Ni(DCO_2)_3$ (a & c) and $ND_4Co(DCO_2)_3$ (b & d) showing the different spin orientations in these two compounds. The spins in $ND_4Co(DCO_2)_3$ are arbitrarily oriented along the a-axis for simplicity and the two differently coloured octahedral in each figure correspond to the two spin orientations in the antiferromagnetic lattice.

1. N. E. Brese and M. O'Keeffe, *Acta Crystallogr.* 1991, **B47**, 192-197.
2. A. S. Antsyshkina, M. A. Porai-Koshits, V. N. Ostrikova and G. G. Sadikov, *Koordinats. Khim.*, 1983, **9**, 855-858.

3. a) G.-C. Xu, W. Zhang, X.-M. Ma, Y.-H. Chen, L. Zhang, H.-L. Cai, Z.-M. Wang, R.-G. Xiong and S. Gao, *J. Am. Chem. Soc.*, 2011, **133**, 14948-14951; b) R. Shang, G.-C. Xu, Z.-M. Wang and S. Gao, *Chem. Eur. J.,* 2014, **20**, 1146-1158;.
4. B. J. Campbell, H. T. Stokes, D. E. Tanner and D. M. Hatch, *J. Appl. Crystallogr.*, 2006, **39**, 607-614.
5. P. Burlet, P. Burlet, J. Rossat-Mignot, A. De Combarieu and E. Bedin, *Phys. Status Solidi B,* 1975, **71**, 675-685.